Combining Small Angle Neutron Scattering (SANS) and Fluorescence Correlation Spectroscopy (FCS) Measurements To Relate Diffusion in Agarose Gels to Structure

Nicolas Fatin-Rouge,*,†,‡ Kevin J. Wilkinson,†,§ and Jacques Buffle†

Analytical and Biophysical Environmental Chemistry, Sciences II, University of Geneva, 30 Quai E. Ansermet, CH-1211 Geneva 4, Switzerland, Laboratory of Material and Interfacial Chemistry, University of Besançon, 25030 Besançon, France, and Department of Chemistry, C.P. 6128, Succursale Centre-ville, University of Montreal, Canada

Received: January 18, 2006; In Final Form: July 27, 2006

Small angle neutron scattering (SANS) and fluorescence correlation spectroscopy (FCS) measurements were carried out on agarose hydrogels to link their microscopic structure to the diffusivity of solutes at different scales. SANS allowed for the determination of the distribution of void volumes within the gels. They were shown to be compatible with a random network of cylindrical fibers as described by the Ogston model. FCS measured solute diffusivity in spaces similar in size to the void volumes, and thus, the results reflected the gel heterogeneity. Solute diffusivity was predicted by modeling the gel as microscopic geometrical cells. Variations in the diffusivity of solutes of different sizes could be predicted from the structural parameters of the gel using theory, taking into account obstruction by cylindrical cells and solute hydrodynamics. Prediction of the FCS autocorrelation functions for solutes from a cell model demonstrated a lack of sensitivity of this technique for multicomponent analysis.

1. Introduction

Agarose is a linear polysaccharide consisting of repeating units of agarobiose (1,3-linked β-D-galactopyranose and 1,4-linked 3,6-anhydro-α-L-galactopyranose) that is isolated from agar extracted from a marine red alga (rhodophyta). Upon cooling of a hot agarose solution in water, double helices[1] of the polymer are formed and aggregated because of hydrogen bonding and hydrophobic interactions. The polymer bundles (or fibers) form a network that entraps water and produces a hydrogel.[2] The porous network has been studied by transmission electron microscopy (TEM),[3] atomic force microscopy (AFM),[4] small angle neutron scattering (SANS),[5,6] and X-ray scattering.[7] These techniques generally show a large pore-size distribution ranging from 1 to 900 nm that depends, among other factors, on the polymer fraction of the gel.[4] The large pore-size distribution and spatial fluctuations of the cross-linking result from the randomness of the cross-linking process.

Diffusion in the agarose gel is of great interest because of the large number of biological, pharmaceutical, and environmental applications.[8,9] For example, agarose gels are widely used for the chromatographic separation of biomolecules because of their high mechanical rigidity, their chemical stability to hydrolysis, and their large average pore size. Until recently, solute interactions with the gel were thought to be mainly of steric nature. It is now known that electrostatic interactions with charged solutes also occur due mainly to the presence of pyruvate moieties on the polymer backbone: the effects of charge on the concentrations and diffusivities of ionic solutes have been recently investigated and modeled.[10] Solute diffusion in gels is still an intense field of research. Nonetheless, the agarose gels are not easy to describe. For example, void volumes are not connected at all scales, and diffusing particles of increasing size sense a decreasing pore connectivity.[11] Therefore, determinations of solute diffusion in gels are still generating intense research interest.

Many diffusion models have been elaborated,[12] but until now, a detailed understanding of the diffusion mechanisms has been largely limited by the fact that models are often compared with diffusion data that have been averaged over the entire porous structure. Porous networks with different void volume distributions can give similar average diffusivities with often substantial experimental errors. To overcome this potential problem, techniques that are sensitive to the local diffusivities of a given solute, indicating variations in local fluctuations of cross-linking densities, must be used. Using a monodisperse solute as a probe, one finds that the distribution of void volume sizes in heterogeneous samples is best reflected by a distribution of diffusion times, in contrast to diffusion in homogeneous media. In this manner, heterogeneous and homogeneous distributions of pore sizes can be distinguished.

Fluorescence correlation spectroscopy (FCS) is a powerful technique used to measure diffusion coefficients (D) under minimally invasive conditions.[13−15] Using laser induced fluorescence and confocal optics, one can correlate concentration fluctuations of extremely dilute solutes at different delay times, τ, following the excitation of a small defined volume called the confocal volume (CV $\sim 10^{-15}$ L; typical dimensions 0.5×3 μm). Temporal autocorrelation curves of the fluorescence intensity fluctuations can be related to diffusion coefficients and kinetic rate constants of processes occurring on time scales of $10^{-7}-10^{2}$ s. In this manner, D values have been obtained for particles in the range 1−300 nm.[16] The technique is extremely useful to investigate diffusion in translucent porous media and interfaces,[11,17] if the size of the CV is comparable to the

* Corresponding author. E-mail: nicolas.fatin-rouge@wanadoo.fr.
† University of Geneva.
‡ University of Besançon.
§ University of Montreal.

10.1021/jp060362e CCC: $33.50
Published on Web 09/13/2006

dimensions of the pores and if measurements are made at stable positions, most often maintained with an antivibration table. In the simplest cases, FCS is used to study samples with one or few diffusing components and the FCS autocorrelation functions (ACF) are analyzed using a single or discrete number of diffusion times, τ_D. However, diffusion-time distributions are increasingly being used to interpret the heterogeneous systems such as those encountered in biological or environmental sciences.[18] In this context, Starchev et al.[19] have interpreted polydispersity using a least-squares fit of the FCS ACF (method of histograms). Using this method, they have reduced the τ_D distribution to a finite number of $\overline{\tau_D}$ with each value being constant over a given interval of D. Independently, Sengupta et al.[20] have used the maximum entropy method to fit their FCS data.

In this paper, we present experimental SANS measurements of cross-link fluctuations in 1.5% agarose gels, which are used to obtain a void volume distribution. The effects of $CaCl_2$ on the cross-linking were also investigated. Void volume distributions were analyzed using a cylindrical cell and other models. Models were tested using diffusivity data for solutes of defined radii. Diffusion time distributions were determined for solutes of increasing sizes on the basis of the distribution of void volumes obtained by SANS. The τ_D distributions were used to predict the FCS ACF of the solutes, acquired over a large number of positions in the gel. The predictions and the sensitivity of FCS ACF to the τ_D distributions are discussed. The combined results provide a rare combination of data describing the gel structure (SANS) and function (FCS), thus providing valuable insight into the physicochemical characteristics of the agarose gel.

2. Theory

2.1. SANS Models: Scattering Functions of Polymer Gels. The exact solution for the scattering function, $I(q)$, has not yet been obtained for cross-linked polymer gels, because local fluctuations of fiber density are very large because of the fractal character of these materials. Nonetheless, the scattering function for a polymer gel can be evaluated by combining scattering of a polymer solution in a semidilute regime and that of a solid.[21−23] Equation 1 is applicable for many polymer gels:[24]

$$I(q) = I_G(0)\exp(-\Xi^2 q^2) + \frac{I_L(0)}{(1+\xi^2 q^2)} \tag{1}$$

where q is the wavenumber, $I_G(0)$ and $I_L(0)$ are the intensities at $q = 0$; and Ξ and ξ are the correlation lengths for the Gaussian and Lorentzian functions, respectively. The former term originates from solidlike heterogeneities and is attributed to correlations inside the polymer bundles; the latter term is attributed to correlations among the polymer bundles in the gel.

Fractal networks are usually characterized by a power law distribution of void volume and solid sizes in space:[25]

$$\bar{m} \propto L^{d_f} \tag{2}$$

where $\bar{m}$ is the average quantity of void volumes or solids in the space volume, averaged over the gel and characterized by a distance L; d_f is the fractal dimension. In the general case, d_f is a fractional number that is smaller than the space dimension of interest. It follows that eq 3 may then be used to describe the scattering of the gel:

$$I(q) = I_B q^{-d_f^B} + I_V q^{-d_f^V} \tag{3}$$

where, as above, I refers to the scattered intensity and the B and V refer to the polymer bundles and void volumes, respectively.

From $I(q)$, it is possible to calculate distance distribution functions, $P(d)$, for intra- and interpolymer bundles from an inverse Fourier transformation of the scattering intensity:

$$P(d) \sim \frac{2}{\pi}\int q\, \mathrm{d}I(q)\sin(qd)\, \mathrm{d}q \tag{4}$$

2.2. Diffusion. In the following, the indices g and w refer to the gel and water phases, respectively. In a hydrogel, the relative diffusivity of a solute relative to water, $\sigma = D_g^s/D_w^s$, is determined by steric, chemical (specific), and electrostatic interactions between the solute and the matrix. In agarose gels, chemical interactions are often weak, and electrostatic interactions can be easily screened by setting an ionic strength larger than 10^{-2} M.[10] When specific and electrostatic interactions are negligible, Brady[26] proposed that σ is given as

$$\sigma = \sigma_{obst} F_C \tag{5}$$

where F_C is the frictional coefficient and σ_{obst} accounts for the obstruction to diffusion. In such a case, the most important parameters to determine the relative diffusivity of a solute in a gel are the hydrodynamic radius of the solute, r_s, the polymer volume fraction in the gel, ϕ, and the partitioning of the free volume with respect to its size distribution and connectivity. The latter parameters are the most difficult to obtain for real materials. Because void volumes are not connected on all size scales, diffusing particles of increasing size sense decreasing pore connectivity. Torquato et al.[27] have introduced the concept of the nearest neighbor distribution function to characterize the void volumes of porous structures. This function allows for the determination of the free volume fraction that is accessible, ϕ_{acc}, for a given solute. In this paper, the porous network is considered to be rigid and immobile.

2.2.1. Obstruction Models. In these models, it is assumed that hydrodynamic interactions are negligible.

2.2.1.1. Ogston/Amsden models. To model the diffusion of solutes of a hydrodynamic radius, r_s, within porous matrixes, it is necessary to introduce ϕ_{acc}, which is the integral of the density distribution function, $g(r)$, of the void volumes of all accessible pores of radius r within the porous material (i.e., for those larger than $2r_s$). Under the assumption that the relative diffusivity of a solute originates only from obstruction effects within a porous network, $\sigma = \sigma_{obst}$, the probability of finding a series of connected void volumes large enough to accommodate the solute is given by[28]

$$\sigma_{obst} = \phi_{acc}(r_s) = \int_{r=r_s}^{\infty} g(r)\, \mathrm{d}r \tag{6}$$

By assuming that polysaccharide gels are random networks of straight, infinitely long cylindrical fibers, Ogston[29] has derived eq 7 to describe the distribution $g(r)$ of spherical void volumes between the polymer fibers:

$$g(r) = \frac{2\phi(r+a)}{a^2}\exp\left[-\phi\left(\frac{r+a}{a}\right)^2\right] \tag{7}$$

After we assume that the fiber thicknesses are negligible compared to their length, eq 7 becomes

$$g(r) = \frac{\pi}{2}\frac{r}{\bar{r}^2}\exp\left[-\frac{\pi}{4}\left(\frac{r}{\bar{r}}\right)^2\right] \tag{8}$$

SCHEME 1

(a)Picture of the agarose gel. (b) Cylindrical cell represents the geometric form of the volume centered on a linear polymer and reproduces the fiber fraction of the hydrogel solution, ϕ, by $\phi = b^2/a^2$.

where a, ϕ, and $\bar{r}$ are the radii of the fibers, their volume fraction in the hydrogel, and the mean radius of the distribution of void volumes, respectively.

The combination of eqs 6 and 8 gives[30]

$$\sigma_{\text{obst}} = \exp\left[-\frac{\pi}{4}\left(\frac{r_s}{\bar{r}}\right)^2\right] \tag{9}$$

This simple mathematical equation works reasonably well for most diffusion data in hydrogels,[28,31−34] using realistic values of the key parameters.

Equation 10 can be obtained from the combination of eqs 6 and 7, given that the porous medium is made of cylindrical fibers and $\phi = (a/(r + a))$:[2]

$$\sigma_{\text{obst}} = \exp\left[-\left(\frac{r_s + a}{\bar{r} + a}\right)^2\right] \tag{10}$$

2.2.1.2. Johansson Cell Model. Using Monte Carlo simulations of Brownian dynamics, Johansson et al.[35] have linked the relative diffusivity of a solute between a network of cylindrical polymer fibers and water with ϕ_{acc}. Among the most descriptive and accurate models,[36,37] σ is obtained from a mesoscopic description of the porous material on the basis of the diffusion flux in microscopic subsystems or cells. In such cases, it is assumed that the structure of porous networks can be decomposed into a set of microscopic elementary cells of a given geometry that contain agarose fibers and solvent (see Scheme 1 for a picture of the agarose gel and the cylindrical cell parameters), through the following relationship:

$$g(r) = \int_a^\infty f(b)\, g^{\text{xc}}(r)\, \mathrm{d}b \tag{11}$$

where $g^{\text{xc}}(r)$ is the probability distribution of spaces of radius r for a cell of a given geometry and $f(b)$ is the distribution function of the cells of radius b. For cylindrical cells, the analytical formulas of $g^{\text{xc}}(r)$ have been derived: [38]

$$g^{\text{cc}}(r) = \frac{2(r + a)}{b^2} S(r - (b - a)) \tag{12}$$

where $S(x)$ is a step function with $S(x) = 1$ for $x \leq 0$ and $S(x) = 0$ for $x > 0$.

Johansson et al.[38] have established an analytical expression for σ_{obst}:

$$\sigma_{\text{obst}} = \int_a^\infty f(b) \frac{D^s(b)}{D_w^s}\, \mathrm{d}b \tag{13}$$

where $D^s(b)/D_w^s$ is the reduced diffusion coefficient of a solute of radius r_s within the elementary cell. The reduced local diffusion coefficient of a spherical particle in a cylindrical cell is[35]

$$\frac{D^s(b)}{D_w^s} = \frac{1}{1 + (r_s + a)^2/b^2} S(r_s - (b - a)) \tag{14}$$

and the probability density of the cells of radius b is

$$f(b) = \frac{2\phi^3 b^3}{a^4} \exp\left(\frac{-\phi b^2}{a^2}\right) \tag{15}$$

Combining eqs 12−15 gives

$$\sigma_{\text{obst}} = \mathrm{e}^{-\eta} + \eta^2 \mathrm{e}^{\eta} E_1(2\eta) \tag{16}$$

with

$$E_1(x) = \int_x^\infty \frac{\mathrm{e}^{-x}}{u}\, \mathrm{d}u \qquad \eta = \phi\left(\frac{r_s + a}{a}\right)^2$$

and $\phi_{\text{acc}}(r_s) = \mathrm{e}^{-\eta}$ Johansson and co-workers have shown that eq 16 is applicable to random polymer networks with a large flexibility[38] (i.e., for polymer persistence lengths $\geq 10a$). In such a case, $g(r)$ can be given by eq 7. Equation 16 has also been determined for other geometries.[39]

2.2.2. Hydrodynamic Models. Hydrodynamic models are based on equations describing the frictional drag that acts on a solute during its transport through a porous material. The models are most often based on the Stokes−Einstein equation by assuming that the solute can be considered a hard sphere that is large compared to the solvent molecules. For example, on the basis of numerical simulations, Clague et al.[40] showed that the frictional drag acting on a spherical solute immersed in a

random suspension of cylindrical fibers of identical radii could be described by

$$F_C(\lambda,\phi) = \exp(-c\phi^d) \tag{17}$$

with $c(\lambda) = 3.727 - 2.460\lambda + 0.822\lambda^2$

and $d(\lambda) = 0.358 + 0.366\lambda + 0.0939\lambda^2$

where λ is the ratio of the fiber radius to solute radius, $\lambda = a/r_s$.[41]

2.3. FCS. The normalized ACF, $G(\tau)$, is defined as[42]

$$G(\tau) = \frac{\overline{\delta F(t) \times \delta F(t+\tau)}}{\overline{F(t)}^2} \tag{18}$$

where t is the acquisition time, τ is the delay time, and $\overline{F(t)}$ is the average fluorescence intensity. The temporal fluctuation intensity, $\delta F(t)$, is defined as

$$\delta F(t) = F(t) - \overline{F(t)} \tag{19}$$

where $F(t)$ is the fluorescence intensity at time t. Physically, $G(\tau)$ corresponds to the probability of detecting, on average, a photon at a delay time, τ, when a photon is detected at $t = 0$. For a single fluorescent species with a low fluorescence intensity with an underfilled objective back-aperture for a one-photon excitation mode,[43] $G(\tau)$ can be given by[44]

$$G(\tau) = \frac{1}{N} G_T(\tau)\left[1 + \frac{\tau}{\tau_D}\right]^{-1}\left[1 + \frac{\tau}{p^2\tau_D}\right]^{-0.5} \tag{20}$$

with

$$G_T(\tau) = \frac{(1 - F_T + F_T \exp(-\tau/\tau_T))}{1 - F_T}$$

where N is the number of fluorescent molecules in the CV, F_T is the triplet fraction, τ_T is the triplet lifetime, p is the ratio between the longitudinal and transverse radii of the CV ($p = \omega_z/\omega_{xy}$), and τ_D is the diffusion time of the fluorescent species in the CV.

D can be estimated from

$$\omega_{xy}^2 = 4D\tau_D \tag{21}$$

where τ_D is the characteristic diffusion time that is spent by the particle in the CV.

In gels, diffusion can be modeled according to two different concepts: the local diffusivity depends (i) on the relative sizes of the solute and the pores or (ii) on the size scale of the pores; the medium can be considered as fractal such that the diffusion is no longer Fickian ("anomalous" diffusion).[45] The average diffusivity results from the different environments.

In (i), if the solute diffuses with a normalized distribution of diffusion times, $h(\tau_D)$, eq 20 can be rewritten:[20]

$$G(\tau) = \frac{G_T(\tau)}{N}\int_{\tau_D^{min}}^{\tau_D^{max}} h(\tau_D)\left[1 + \frac{\tau}{\tau_D}\right]^{-1}\left[1 + \frac{\tau}{p^2\tau_D}\right]^{-0.5} d\tau_D \approx G_T(\tau)\sum_{i=1}^{\zeta} c(\tau_{Di})\Delta\tau_{Di}\left[1 + \frac{\tau}{\tau_D}\right]^{-1}\left[1 + \frac{\tau}{p^2\tau_D}\right]^{-0.5} \tag{22}$$

where τ_D^{min} and τ_D^{max} are the shortest and longest diffusion times of the distribution, $c(\tau_{Di})$ is the discrete distribution of diffusion times, and $\sum_{i=1}^{\zeta} c(\tau_{Di})\Delta\tau_{Di} = 1/N$. τ_D^{min} provides an estimation of the average diffusion time of the solute in water, because it corresponds to its diffusion in a void volume that is much larger than its size where its interactions with the gel can be neglected. The second half of eq 22 is useful because analytical solutions are scarce for the former relationship.

In (ii), eq 20 is modified to account for anomalous diffusion[11] by raising τ/τ_D to the exponent α (anomalous exponent)[46] to account for the broadening of the FCS ACF in heterogeneous media as compared to what is observed in homogeneous media.

$$G(\tau) = \frac{1}{N} G_T(\tau)\left[1 + \left(\frac{\tau}{\tau_D}\right)^{\alpha}\right]^{-1}\left[1 + \frac{1}{p^2}\left(\frac{\tau}{\tau_D}\right)^{\alpha}\right]^{-0.5} \tag{23}$$

3. Experimental Section

Gels and Reagents. Purified agarose (LGL, molecular biology grade, Biofinex, Switzerland, lot no. 8041) was used without further treatment. For SANS measurements, 1.5% w/w agarose, corresponding to a polymer fraction (ϕ) of 0.0137[47] was dissolved in warm (80 °C) D_2O before its slow cooling to room temperature. D_2O solutions of $CaCl_2$ (thoroughly dried to remove H_2O) were used in some gel preparations to study the influence of Ca^{2+} on the gel structure. For FCS measurements, gels were prepared in a similar manner except that D_2O was substituted with H_2O. Aqueous solutions of rhodamine 6G (R6G), alexa-488 labeled codfish parvalbumin, and R-phycoerythrin were prepared as described previously.[11] All solutions could be well-fitted by a single-component FCS ACF.

SANS Experiments. SANS measurements were carried out at the Swiss Spallation Neutron Source (Paul Scherrer Institute). Experiments were performed at three detector positions (2, 8, 20 m) to work with the full q range available, $0.0177 \le q \le 2$ nm^{-1}. Experimental scattering data were radially averaged to obtain differential cross-sections, $I(q) = d\Sigma(q)/d\Omega(q)$, which were then analyzed for $q \le 0.6$ nm^{-1} (see Figure 1b).

Measurement of Diffusion Times by FCS. Diffusion times of solutes and particles in the agarose gel were measured by fluorescence correlation spectroscopy (ConfoCor Axiovert 135 TV; Carl Zeiss), using a 50 μm pinhole. A water immersion 40× objective and inverted microscope were employed. Various fluorophores were added to the gel, before excitation with an Ar ion (488 or 514 nm) or a He/Ne laser (545 nm). The fluorescence intensity was measured with an avalanche photodiode (SPCM-200PQ). Fluorescence intensity variations in the CV are attributed to the translational diffusion of the fluorescent particles. Values of p, ω_{xy}, and ω_z were obtained by calibration with R6G, which has a known diffusion coefficient of 2.8×10^{-6} cm^2 s^{-1} at 20 °C in water.[15] Artifacts due to the non-Gaussian nature of the CV were minimized and verified by calibration. In this work, only one-component systems have been employed to focus on τ_D distributions that were due to the diffusion of finite-sized solutes within the gel. For each fluorescent particle, the FCS ACF was recorded at 40 different positions within the gel sample to ensure representivity of the diffusion measurements. Acquisition times of 200 s were used to optimize the signal-to-noise ratio.

Numerical Simulations. Numerical simulations were made using Matlab or Maple. Fits of the FCS ACF with a single τ_D or a τ_D distribution were processed with eqs 20, 22, or 23. τ_{Dg}^s distributions, accounting for obstruction and hydrodynamics, were obtained by applying the density of the reduced local diffusivity to a single diffusion time, τ_{Dw}^s. For each solute, τ_{Dg}^s distributions were shifted to obtain the lowest residuals. Gener-

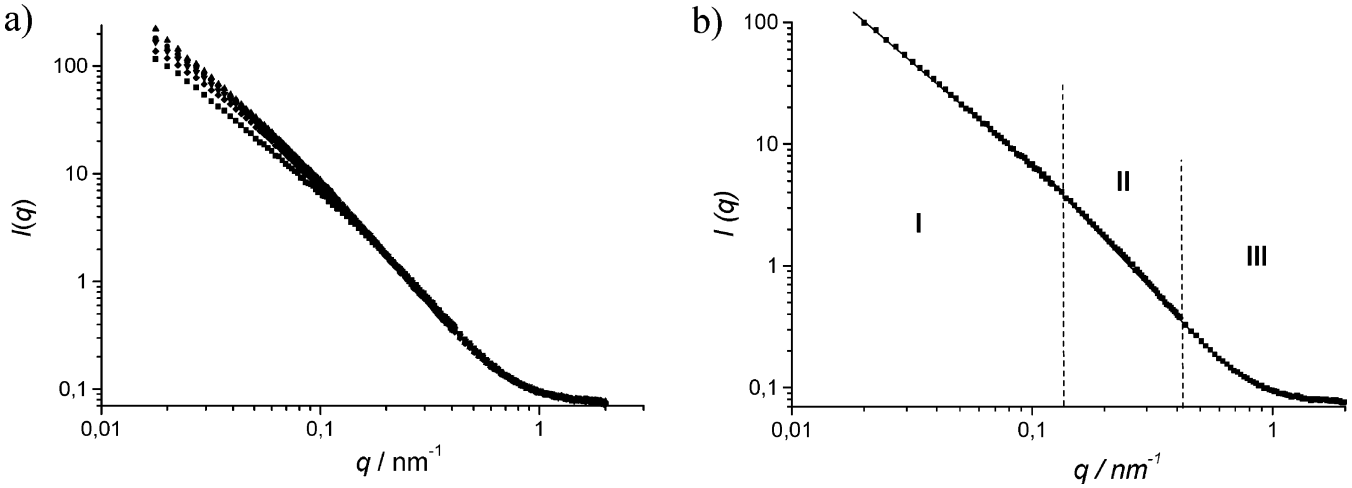

Figure 1. SANS intensities, $I(q)$, of a 1.5% agarose hydrogel. (a) $I(q)$ for $[CaCl_2] = 0$ (■), 0.01 (●), 0.05 (▲), 0.10 (▼), 0.50 (◆), 1.00 M (+). (b) $I(q)$ without $CaCl_2$. Slopes are $\gamma = 1.69$ (domain I) and $d_f^B = 2.11$ (domain II) as obtained with the fractal analysis. $T = 20$ °C.

ally, the fastest diffusion time obtained for the distribution, τ_{D0}^s, was very close to τ_{Dw}^s.

4. Results and Discussion

4.1. SANS Measurements: Effects of [Ca^{2+}] and Ionic Strength (μ) on the Gel Structure. SANS intensities of 1.5% w/w agarose hydrogels are presented in Figure 1a for various concentrations of $CaCl_2$. Data were not analyzed at high values of q, because scattering was incoherent, likely due to the hydrogen bound to the agarose itself, whereas the model used here assumes that neutrons were scattered only by polymer bundles and void volumes. Spectra were superimposed by taking the values $I(q=2)$ as a reference. Scattering spectra displayed continuous and smooth variations without intensity maxima, but the continuous increase at low q provided some evidence for cross-linking, an observation that would not occur in polymer solutions. This result is typical for low functionality gels, e.g., for gels formed by random cross-linking of long linear chains in semidilute solutions (i.e., statistical gels).[48] The lack of a maximum (i.e., lack of correlation length) is likely due to the polydispersity of the cluster sizes and to the cross-linking.[48] Indeed, TEM observations[49] have shown a 3D randomly structured network with pore sizes ranging from tens to thousands of nanometers. These images suggest that the data would be best analyzed by a fractal model of a random distribution of self-similar junctions of different lengths. Three main regions can be observed for each agarose sample: domain I corresponding to a length scale of 40−350 nm ($I(q) \propto q^{-\gamma}$, $q = 0.0177-0.15$ nm^{-1}), domain II corresponding to a length scale of 10−40 nm ($I(q) \propto q^{-d_f^B}$, $q = 0.15-0.7$ nm^{-1}), and domain III corresponding to a length scale of 3−10 nm ($q \geq 0.7$ nm^{-1}) (Figure 1b). Some changes were observed at low q for [Ca^{2+}] between 0 and 0.01 M, but only minor changes were observed above 0.01 M Ca^{2+} (Figure 1a). Such a result is consistent with a complete screening of the charges on the agarose gel (concentration of anionic sites in the gel is 8.8×10^{-4} mol/L)[10] for ionic strengths above 0.01 M.

Experimental values of the scattering exponents were $\gamma = 1.79 \pm 0.09$ and $d_f^B = 2.110 \pm 0.004$. On the basis of a model of uncorrelated compact fractal domains,[50,51] $\gamma = d_f^B(3 - \theta)$, where θ is the polydispersity index of the mass distribution of agarose aggregates, $P(M) \propto M^{-\theta}$.[52] The value of γ was typical for statistical gels[48] and was in agreement with previous results obtained for agarose.[5] Theoretical d_f values of 2.5, 2.1, and 1.8 are expected for percolation, reaction-limited aggregation, and diffusion-limited aggregation, respectively. The experimental value of $d_f = 2.11$ suggests that the reaction-limited aggregation model is most appropriate, leading to a polydispersity index, θ, of 2.14 ± 0.04. Within experimental error, γ and θ were not correlated with [Ca^{2+}] (Table 1).

TABLE 1: Fractal Exponent (γ) and Polydispersity Index of the Mass Distribution of Agarose Bundles (θ) As Obtained from the Fractal Analysis of Experimental $I(q)$ vs [$CaCl_2$][a]

$[CaCl_2]/M$	γ	θ
0	1.715(7)	2.183(3)
0.01	1.81(2)	2.138(9)
0.05	1.88(1)	2.105(5)
0.1	1.78(2)	2.152(9)
0.5	1.74(2)	2.171(9)
1	1.81(2)	2.138(9)

[a] Agarose/D_2O: 1.5% w/w; $T = 20$ °C.

Estimation of the average correlation lengths Ξ and ξ were obtained by analyzing the entire scattering intensity profiles with eq 1. The structure of the agarose hydrogel may be considered like domains of high density, cross-linked polymers that are separated by pores and form an overall low-density network. ξ can be roughly considered as the pore size, and Ξ can be interpreted as the size of the high density, cross-linked domains. Figure 2 shows how these two parameters are affected by $[CaCl_2]$. The experimental value of $\xi \sim 70$ nm was in good agreement with a previous estimation of the average pore diameter that was obtained from diffusion measurements.[10] In the absence of Ca^{2+} (arbitrarily set at 10^{-5} M in Figure 2), a value of 5.9 nm was obtained for Ξ, and for $[Ca^{2+}] \geq 10^{-2}$ M, Ξ was equal to 15 ± 2 nm. These values were consistent with previously reported X-ray diffraction data on agarose gels in which correlation lengths of 3 and 9 nm were attributed to the double helices of agarose and their cross-linking, respectively.[7] Variations of Ξ with [Ca^{2+}] suggested that calcium may favor cross-linking due to a charge screening.

To relate the diffusivity of solutes in the gel with the gel structure, it is necessary to analyze the porous structure as a void volume distribution. In this optic, the distance distribution function, $P(d)$, is useful for the interpretation of correlations both within and among agarose bundles. $P(d)$ was calculated by combining eq 4 with either eq 1 or 3 (Figure 3). The two models gave very similar distribution functions of the void volumes ($\overline{\varnothing}_{cavity} = 45$ nm), although the Geissler model (eq 1) gave a slightly larger length for the agarose bundle distribution

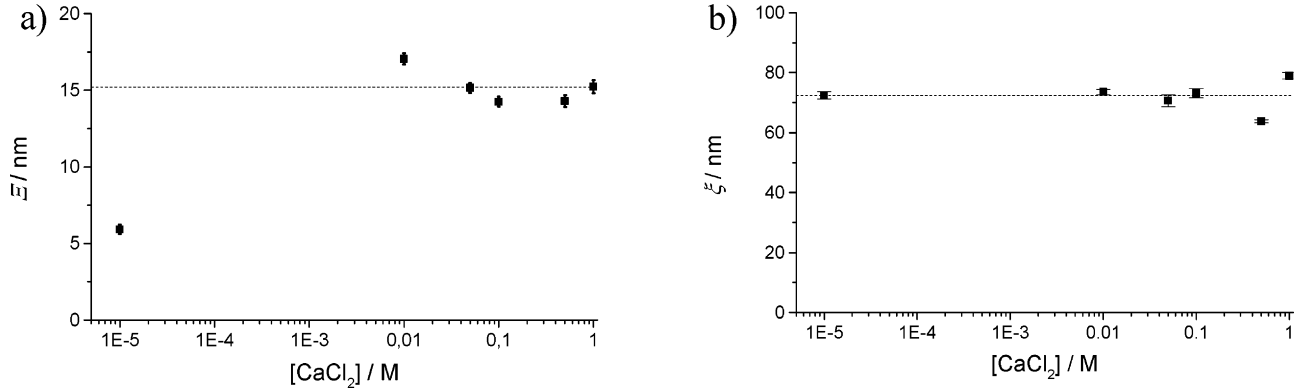

Figure 2. Correlation lengths Ξ and ξ for polymer bundles and pores as a function of the concentration of $CaCl_2$.

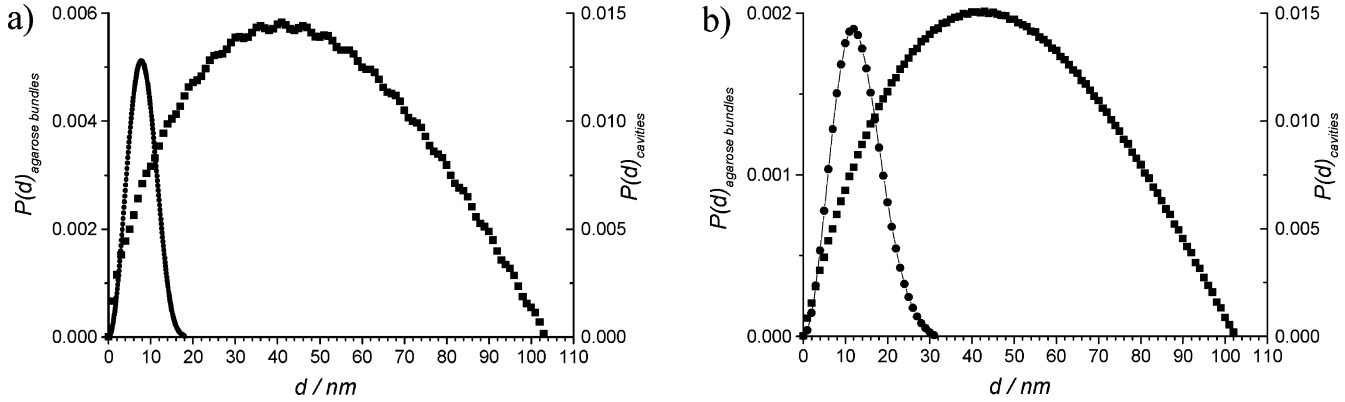

Figure 3. Distance distribution functions for intra- (●) and inter- (■) agarose bundle correlations, $P(d)$, for 1.5% agarose hydrogels free of Ca^{2+}. $P(d)_{cavities}$ have been normalized. (a) Values obtained from the power law fractal analysis (eq 3) of $I(q)$. (b) Values obtained from Geissler modeling (eq 1) of $I(q)$. $T = 20$ °C.

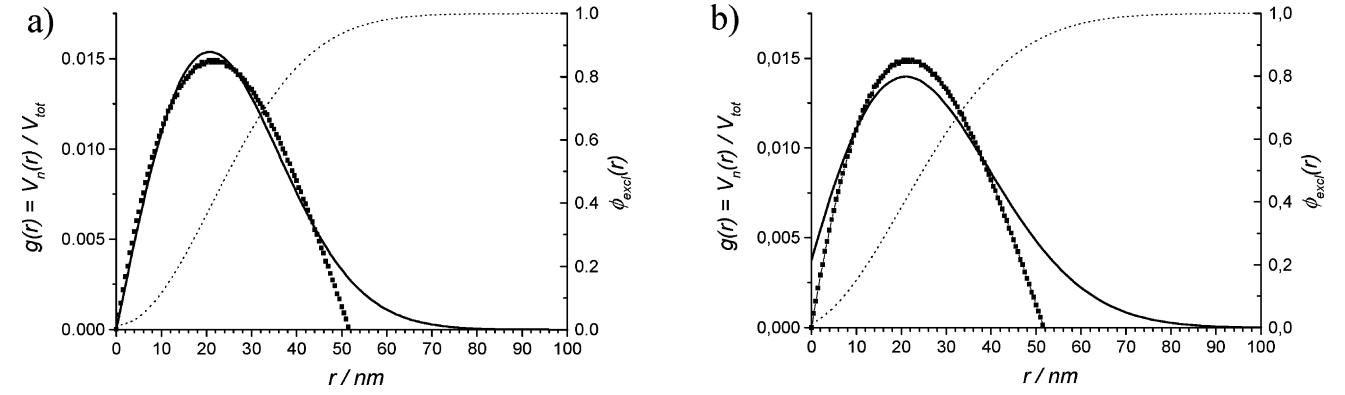

Figure 4. Experimental probability distribution of spherical void volumes (i.e., neighbor void volume fraction, $V_n(r)/V_{tot}$) as a function of radius, r, as deduced from SANS experiments (■). Experimental data were fitted with (a) eq 8 (bold solid line, $\bar{r} = 26.7$ nm) (b) an Ogston distribution, eq 7 (bold solid line, $\phi = 0.0137$, $a = 4.1$ nm). ϕ_{exc} vs r_s was calculated from the integral of the distribution functions (dotted lines).

($\overline{\varnothing}^{\text{Geissler}}_{\text{bundle}} = 13$ nm) as compared to the Fractal model ($\overline{\varnothing}^{\text{Fractal}}_{\text{bundle}} = 8$ nm). The presence of Ca^{2+} concentrations that were in excess with respect to the pyruvate functional groups resulted in an increase in the size of the agarose bundles (Geissler model, Figure S1, $\overline{\varnothing}^{\text{Geissler}}_{\text{bundle}} = 32$ nm), with no effect on the pore-size distribution.

4.2. Average Diffusion Coefficients and Microscopic Models. *Mathematical Analysis of SANS Void Volume Size Distribution.* In the present section, the normalized experimental distribution of void volumes presented in Figure 3b was used to calculate macroscopic diffusion coefficients of solutes. In a first step, SANS results of the normalized void volume size distributions have been analyzed using different mathematical models. On the basis of AFM[4] and TEM[3] studies, the presence of void volumes, up to about 1 μm in diameter, is expected. The experimentally determined normalized distribution of void volumes fitted with mathematical equations describing distributions $g(r)$ of cells that were centered around infinitely long cylinders of real (eq 7) or negligible (eq 8) sizes (Figure 4).[53] In Figure 4, the excluded volume fraction, ϕ_{exc}, was also calculated[54] and plotted against the radius of a diffusing particle for each of the models. The experimental $g(r)$ values obtained by SANS are well described as a random array of cylindrical fibers using either eq 7 or 8 for $r \leq 40-50$ nm. Such a result is not completely unexpected because, under the present experimental conditions, SANS is not very sensitive at low and high q values (i.e., for $r \sim 0$ or $r \geq 50$ nm). Although eq 8 appears to fit $g^{SANS}(r)$ data slightly better than eq 7 does, ϕ and $a = 0$ do not correspond to physically realistic conditions. Nonetheless, the critical radius, r_c, defined as the lowest r value

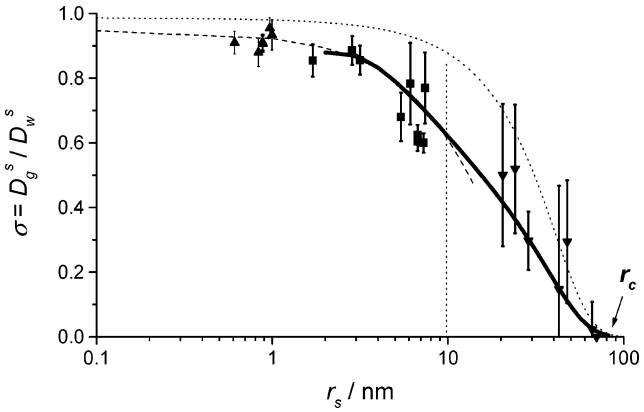

Figure 5. σ vs r_s for R6G, NileBlue, humic, and fluvic acids (▲), proteins (■), latex beads (▼), which have been shown to display only steric interactions with the agarose gel.[10,11] pH = 7.0 (phosphate buffer); T = 20 °C. Data were predicted from the Johansson equation (eq 16, dotted line, ϕ = 0.0137, a = 4.1 nm), and from the product of the Johansson and Clague equations (eqs 16 and 17, bold solid line, ϕ = 0.0137, a = 4.1 nm). The dashed line is the prediction that is obtained for $r_s \leq 10$ nm from eqs 14 and 24.

for which $\phi_{exc}(r) > 99\%$ (i.e., minimum size of a completely trapped particle) was determined to be ~80 or 90 nm, respectively, in excellent agreement with prior diffusivity results for this gel.[11] In addition, parameters extracted from these fits (a = 4.1 nm, eq 7 and $\bar{r}$ = 26.7 nm, eq 8) were in good agreement with the average "diameters", $\overline{\varnothing}^{\text{Fractal}}_{\text{bundle}} = 8$ nm and $\overline{\varnothing}_{\text{cavity}} = 45$ nm, extracted from SANS measurements (above). Because of the different length scales in the gel, a cannot be simply considered as the radius of a single double helix of agarose but rather should be considered as the average radius of the different solid objects within the gel.

Macroscopic Diffusion Coefficients—Diffusion Models. The Amsden and Johansson obstruction models and the hydrodynamic model developed by Clague[40] were tested by comparing model prediction with experimental results of relative diffusivity, σ, obtained from FCS experiments[11] using a wide range of solute sizes that were on the same order of magnitude as the pore sizes. Only solutes exhibiting steric interactions with the gel (i.e., no chemical interactions) are reported (Figure 5, Figure S2). For r_s values that were close to the $\bar{r}$ value of 26.7 nm, spatial variations of σ values were large, because the void volume connectivity was small and the probability of being adjacent to a neighboring void volume of equal or larger size was very low. The main conclusions that could be drawn from the models follow: (i) From eq 10 and values of $\phi_{exc}(r)$ (Figure 4b), σ vs r_s is predicted to decrease more rapidly with decreasing a (Figure S2a, the best χ^2 value obtained from these fits is 0.41, for a = 2 nm). By taking into account distributions of a that were extracted from SANS, it was possible to improve the model prediction, but no model was satisfactory over the entire range of solute sizes. (ii) Reasonable structural values were obtained using the Amsden models, but σ predictions were poor (Figure S2b). The use of eq 10 (with set parameters $\bar{r}$ = 27.6 nm and a = 3.2 nm) slightly improved the prediction of the intermediate values of r_s, though it was still unsatisfactory (χ^2 = 0.42). (iii) Finally, the Johansson equation (eq 16) was used to predict σ values (Figure 5, dotted line) without any adjusted parameters from the known values of a and ϕ (i.e., $\phi_{acc}(r)$). σ values were overestimated over the entire range of r_s, strongly suggesting that, in addition to obstruction effects, hydrodynamic interactions needed to be taken into account. Indeed, when both effects were considered by using the product of σ_{obst} (eq 16) and F_C (eq 17), it was possible to greatly improve the fit with the data (Figure 5, solid line, χ^2 = 0.10) without any adjusting parameters. Nonetheless, an important limitation of eq 17 is that F_C cannot be predicted for $r_s \leq 2$ nm, a limit fixed by the value of a. Another limitation of the cell model is that the parameters in eq 17 are obtained by an averaging process over many local configurations. For example, the parameter λ has no physical meaning with respect to the size of the cells.

TABLE 2: $\overline{\tau_D^s}$ Values (ms) for Three Solutes As Measured from the FCS ACF with a Single Diffusion Time or Calculated from $\tau_{Dw}^{s\_FCS}$ and $D^s(b)/D_w^s$ in Cylindrical Cells[a,b]

solute	p	ω_{xy}/nm	$\tau_{Dw}^{s\_FCS}$	$\overline{\tau_{Dg}^{s\_FCS}}$	$\overline{\tau_{Dg}^{s\_cc}}$
R6G	7.308	230	0.0475	0.0522	0.0493
paravalbumin	6.405	255	0.224	0.262	0.263
R-phycoerythrin	6.059	280	0.672	0.872	0.921

[a] Equations 14, 15, and 24. [b] Agarose/H_2O: 1.5% w/w; pH = 7.0; μ = 0.01 M; T = 20 °C.

Given the heterogeneity of the gel, a cell model that describes D distributions in agarose on a microscopic scale would likely be more appropriate to test against the experimental FCS ACF. Because the average relative diffusivity (eq 5) could be accurately predicted from σ_{obst}[4] in the r_s range of 2−10 nm and below (Figure 5), a similar relationship was derived to describe the reduced diffusivity, $D(b)/D_w$ on a microscopic scale:

$$\frac{D^s(b)}{D_w^s} = \left(\frac{D_{obst}^s(b)}{D_w^s}\right)^4 \tag{24}$$

In the next section, both a Fickian (eq 20) and an anomalous (eq 23) one-component analysis of the experimental FCS ACF averaged over a large number of positions in the gel will be compared with distributions obtained from eqs 22 and 24.

4.3. FCS ACF. τ_D^s *Distributions in Agarose Gel.* The probability density of the reduced diffusivities in cylindrical cells, $f(b)$, and the corresponding reduced diffusivities were determined from eqs 14, 15, and 24. Even for solutes with a single discrete diffusion time in water, a distribution of diffusion times was observed in the gel because of the pore size polydispersity. On the basis of knowledge of τ_{Dw}^s, $D^s(b)/D_w^s$, and $f(b)$, FCS ACF curves in the gel were predicted for three solutes of variable sizes: R6G (r_s = 0.8 nm), parvalbumin (r_s = 3.2 nm), and R-phycoerythrin (r_s = 7.4 nm). In each case, r_s values were deduced from the Stokes−Einstein equation. These solutes were selected for various reasons: (i) They were chemically pure and monodisperse (i.e., no size distribution).[18,19,55,56] (ii) Their size was negligible compared to ω_{xy} such that no correction was required to account for finite size effects in the mathematical expression of the ACF.[16,55] (iii) These solutes have only steric interactions with the agarose gel.[11] In the gel, diffusivity distribution arises from obstruction to solute diffusion and hydrodynamics in the microscopic void volumes of the gel. Normalized τ_{Dg}^s distribution obtained as $\tau_{Dw}^s(D_w^s/D^s(b))$ (Figure S3) with the corresponding probability were used to calculate the ACF FCS, and the $\overline{\tau_{Dg}^s}$ values obtained from eqs 14, 15, and 24 are reported in Table 2 for comparison with the one-component analysis. Differences between $\overline{\tau_{Dg}^s}$ values are < 5.5% (case for the largest solute examined, R-phycoerythrin). For R-phycoerythrin, $\alpha < 0.9$, and eq 20 becomes inappropriate to model the ACF FCS.

The experimental FCS ACF for the three solutes in the agarose gel were fitted to the ACF generated by eqs 20, 22, and 23 and based upon the diffusion times in water (Figure 6). The least-squares fits generally followed the sequence χ^2 (single-

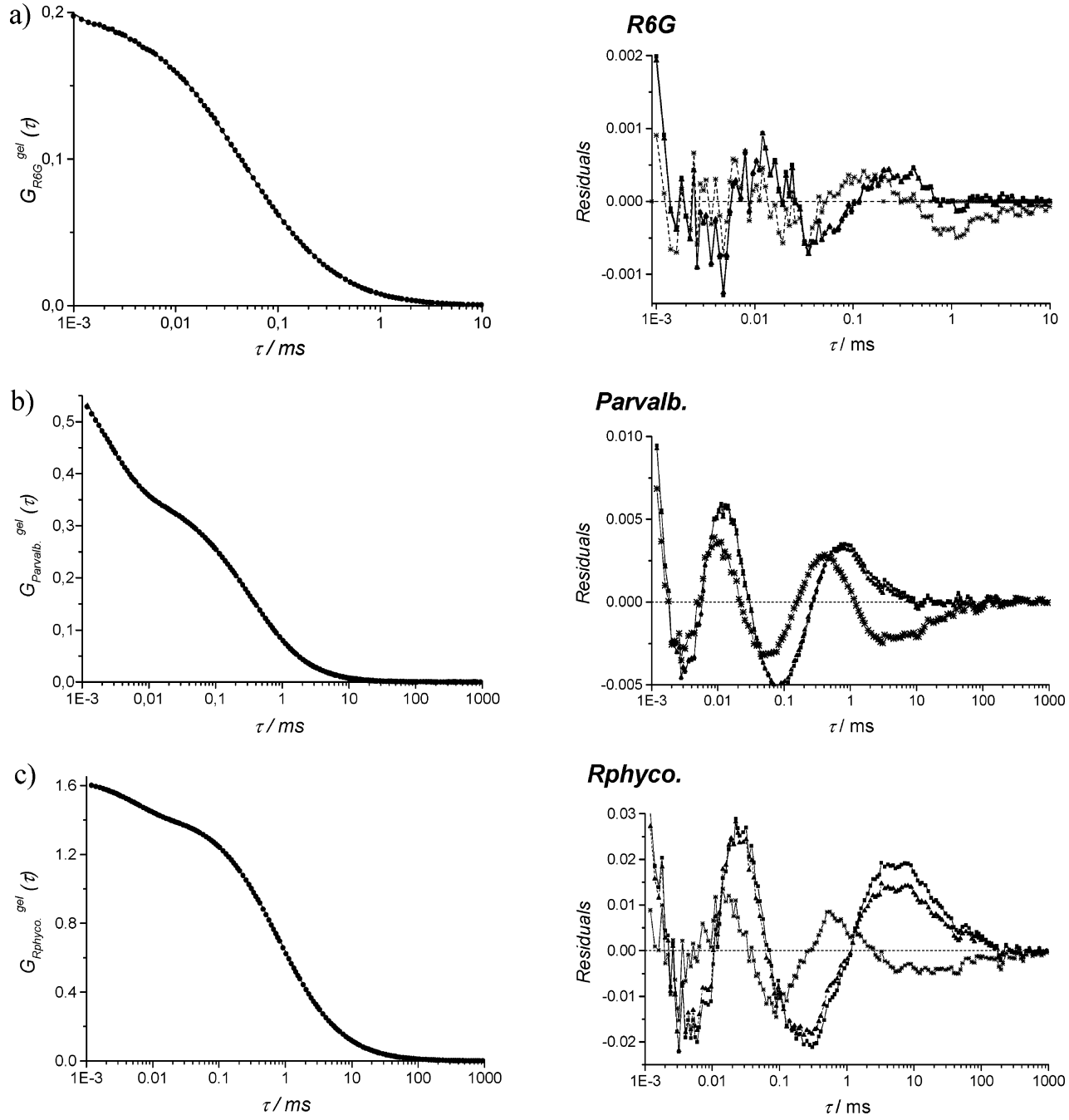

Figure 6. Averaged FCS ACF of diffusing solutes in 1.5% agarose gel (left) and residuals of the fits (right). Fit with a single component: eq 20 (■), eq 23 (∗) anomalous diffusion. Fit with τ^{s}_{Dg} distributions beginning at the shortest diffusion time τ_0 (ms): eqs 22 and 24 (▲). (a) R6G: $\chi^2_{■} = 1.82 \times 10^{-5}$; $\chi^2_{*} = 1.11 \times 10^{-5}$, $\alpha = 0.965$, $\tau_D = 0.0469$; $\chi^2_{▲} = 1.76 \times 10^{-5}$, $\tau_0 = 0.0488$. (b) Parvalbumin: $\chi^2_{■} = 1.12 \times 10^{-3}$; $\chi^2_{*} = 5.57 \times 10^{-4}$, $\alpha = 0.930$, $\tau_D = 0.277$; $\chi^2_{▲} = 1.04 \times 10^{-3}$, $\tau_0 = 0.263$. (c) R-phycoerythrin: $\chi^2_{■} = 2.99 \times 10^{-2}$; $\chi^2_{*} = 4.79 \times 10^{-3}$, $\alpha = 0.894$, $\tau_D = 0.771$; $\chi^2_{▲} = 2.25 \times 10^{-2}$, $\tau_0 = 0.653$.

component Fickian diffusion) > χ^2 (τ^{s}_{Dg} distributions) > χ^2 (anomalous diffusion). In contrast, because residuals were differently distributed for R-phycoerythrin, it was concluded that eq 23 was the most appropriate equation to fit FCS ACF in heterogeneous media. χ^2 values could be improved further with respect to a single-component analysis by increasing the weighting of the large τ_D values (factor of ≥2 for parvalbumin and ≥4 for R-phycoerythrin) and maintaining $\overline{\tau^{s}_{Dg}}$ constant, in particular for large r_s. Apparently, local diffusion coefficients are more dependent on b (eq 24) than has been assumed previously; this could also be the case because eq 24 was not able to correctly take into account hydrodynamics. Finally, the FCS technique itself was not very sensitive to differences in τ_D distributions, an observation that has been noted previously.[20,57,58]

5. Conclusion

The structure of an agarose gel has been investigated and successfully modeled by the random stacking of cylindrical fibers. The size distribution of void spaces was described, and the accessible volume fraction and the average size of agarose bundles was determined. Although several diffusion models were tested to predict the average diffusion coefficients in the gel, only a combination of models accounting for obstruction

in cylindrical cells (Johansson) and hydrodynamics (Claque) were able to accurately predict σ vs r_s data in the agarose gel. τ^s_{Dg} distributions were obtained by using a cell model that was accurate for determining average values; however, FCS was shown to have a low sensitivity to τ_D distributions.

Acknowledgment. We thank Dr. V. Aswal for his assistance with SANS measurements. This work was supported by grants from the Swiss National Science Foundation.

Glossary

a: radius of polymer fibers

b: cell radius in the microscopic cell model theory

d_f: mass fractal dimension

d_w: fractal exponent of diffusion

cc: cylindrical cell

D: diffusion coefficient (subscripts g (gel), w (water); superscript refers to particle)

$f(b)$: distribution function of cells of radii b

F: fluorescence intensity

F_C: frictional coefficient

F_T: triplet fraction

$g(r)$: distribution function of void spaces of radii r

I: SANS scattered intensity

L: linear size

$\bar{m}$: average quantity

N: mean number of particles in the confocal volume

p: FCS structure parameter of the confocal volume

$P(d)$: distance distribution function of intra- or interpolymer bundles

q: wavenumber, $q = (4\pi \sin(\varphi/\lambda))$, where 2φ is the scattering angle

$\bar{r}$: average pore radius of a porous material

$\bar{r}_{obs}$: average radius of obstacles in a porous medium

r_s: hydrodynamic radius of diffusing particles

r_c: critical radius (i.e., the minimum size of completely trapped particles within the gel)

t: time

α: anomalous exponent of diffusion

γ: fractal exponent

δ_F: fluctuation of fluorescence intensity

ϕ: volume fraction of fibers in the gel. For agarose, its calculation has been explained in ref 47.

λ: ratio of the fiber radius to solute radius

μ: ionic strength (/M)

σ: reduced diffusion coefficient in a porous medium

θ: polydispersity index of a mass distribution

τ: delay time

τ_D: diffusion time

τ^s_{Dw}, τ^s_{Dg}: diffusion times of solute s in water and in gel, respectively

τ_T: triplet time

ξ: correlation length of pores or network mesh size

Ξ: correlation length of fibers

ω_z, ω_{xy}: longitudinal and transverse radii of the CV, respectively

Supporting Information Available: A plot for distance distributions functions for aggregates and cavities in the presence of Ca^{2+} ions, variations of experimental relative diffusivity for various solutes as a function of their size using obstruction models, density probability of reduced local diffusivity for various solutes as a function of their size. This material is available free of charge via the Internet at http://pubs.acs.org.

References and Notes

(1) Arnott, S.; Fulmer, A.; Scott, W. E.; Dea, C. M.; Moorhouse, R.; Rees, D. A. *J. Mol. Biol.* **1974**, *90*, 269−284.
(2) Rees, D. A. *Carbohydr. Chem. Biochem.* **1969**, *24*, 267−332.
(3) Waki, S.; Harvey, J. D.; Bellamy, A. R. *Biopolymers* **1982**, *21*, 1909−1926.
(4) Pernodet, N.; Maaloum, M.; Tinland, B. *Electrophoresis* **1997**, *18*, 55−58.
(5) Krueger, S.; Plopis Andrews, A.; Nossal, R. *Biophys. Chem.* **1994**, *53*, 85−94.
(6) Deriu, A.; Cavatorta, F.; Cabrini, D.; Middendorf, H. D. *Prog. Colloid Polym. Sci.* **1991**, *84*, 461−464.
(7) Djabourov, M. A.; Clark, H. A.; Rowlands, D. W.; Ross-Murphy, S. B. *Macromolecules* **1989**, *22*, 180−188.
(8) Ottenbrite, R. M.; Huang, S. J. *Hydrogels and Biodegradable Polymers for Bioapplications*; Park, K., Ed.; American Chemical Society: Washington, DC, 1996.
(9) Buffle, J. *Complexation Reactions in Aquatic Systems—An Analytical Approach*; Wiley & Sons: New York, 1988.
(10) Fatin-Rouge, N.; Milon, A.; Buffle, J.; Goulet, R. R.; Tessier A. *J. Chem. Phys. B* **2003**, *107*, 12126−12137.
(11) Fatin-Rouge, N.; Starchev, K.; Buffle, J. *Biophys. J.* **2004**, *86*, 2710−2719.
(12) Masaro, L.; Zhu, X. X. *Prog. Polym. Sci.* **1999**, *24*, 731−775.
(13) Magde, D.; Elson, E. L.; Webb, W. W. *Phys. Rev. Lett.* **1972**, *29*, 705−708.
(14) Elson, E.; Magde, D. *Biopolymers* **1974**, *13*, 1−27.
(15) Madge, D.; Elson, E.; Webb, W. W. *Biopolymers* **1974**, *13*, 29−61.
(16) Starchev, K.; Zhang, J. W.; Buffle, J. *J. Colloid Interface Sci.* **1998**, *203*, 189−196.
(17) Study of environmental systems by fluorescence correlation spectroscopy: Fatin-Rouge, N.; Buffle, J. In *Environmental, Analytical, and Physical Chemistry*; Wilkinson, K., Lead, J., Eds.; IUPAC Series; Wiley-Interscience: Cambridge, U.K.; Vol. 5, to be published.
(18) Lead, J. R.; Wilkinson, K. W.; Balnois, E.; Cutak, B. J.; Larive, C. R.; Assemi, S.; Beckett, R. *Environ. Sci. Technol.* **2000**, ***34***, 3508−3513.
(19) Starchev, K.; Buffle, J.; Perez, E. *J. Colloid Interface Sci*. **1999**, *213*, 479−487.
(20) Sengupta, P.; Garai, K.; Balaji, J.; Periasamy, N.; Maiti, S. *Biophys. J.* **2003**, *84*, 1977−1984.
(21) Hecht, A. M.; Duplessix, R.; Geissler, E. *Macromolecules* **1985**, *18*, 2167−2173.
(22) Mallan, S.; Horkay, F.; Hecht, A. M.; Geissler, E. *Macromolecules* **1989**, *22*, 3356−3361.
(23) Horkay, F.; Hecht, A. M.; Mallan, S.; Geissler, E.; Renie, A. R. *Macromolecules* **1991**, *24*, 2896−2902.
(24) Shibayama, M.; Tanaka, T. *J. Chem. Phys.* **1992**, *97*, 6829−6841.
(25) Havlin, S. Molecular Diffusion and Reactions. In *The Fractal Approach to Heterogeneous Chemistry*; Avnir, D., Ed.; Wiley & Sons: New York, 1989; pp 251−269.
(26) Brady, J. F. Hindered diffusion. In *Extended Abstracts, American Institute of Chemical Engineers Annual Meeting*, San Francisco, CA, 320.
(27) Torquato, S.; Lee, S. B. *Physica A* **1990**, *167*, 361−383.
(28) Amsden, B. *Macromolecules* **1998**, *31*, 8382−8395.
(29) Ogston, A. G. *Trans. Faraday Soc.* **1958**, *54*, 1754−1757.
(30) Amsden, B. Solute Diffusion in Hydrogels. *Polym. Gels Networks* **1998**, *6*, 13−43.
(31) Amsden, B. *Polymer* **2002**, *43*, 1623−1630.
(32) Amsden, B. *Macromolecules* **1999**, *32*, 874−879.
(33) Amsden, B. *Macromolecules* **2001**, *34*, 1430−1435.
(34) Amsden, B. *Macromolecules* **2002**, *35*, 3179−3183.
(35) Johansson, L.; Elvingson, C.; Löfroth, J. E. *Macromolecules* **1991**, *24*, 6019−6023.
(36) Jönsson, B.; Wennerström, H.; Nilsson, P. G.; Linse, P. *Colloid Polym. Sci.* **1986**, *264*, 77−88.
(37) Nilsson, L. G.; Nordenskiöld, L.; Stilbs, P.; Braulin, W. *J. Phys. Chem.* **1985**, *89*, 3385−3391.
(38) Johansson, L.; Elvingson, C.; Löfroth, J. E. *Macromolecules* **1991**, *24*, 6024−6029.
(39) Netz, P. A.; Dorfmüller, T. *J. Chem. Phys.* **1997**, *107*, 9221−9233.
(40) Clague, D. S.; Phillips, R. J. *Phys. Fluids* **1996**, *8*, 1720−1731.
(41) Phillips, R. J. A. *Biophys. J.* **2000**, *79*, 3350−3353.
(42) Webb, W. W. *Q. Rev. Biophys.* **1976**, *9*, 49−68.
(43) Hess, S.; Webb, W. W. *Biophys. J.* **2003**, *83*, 2300−2317.

(44) Aragon, S. R.; Pecora, R. *J. Phys. Chem.* **1976**, *64*, 1791−1803.

(45) Netz, P. A.; Dorfmüller, T. *J. Phys. Chem.* **1995**, *103*, 9074−9082.

(46) Schwille, P.; Korlach, J.; Webb, W. W. *Cytometry* **1999**, *36*, 176−182.

(47) The volume fraction of agarose is obtained as $\phi = (C_{agarose}/\rho^{agarose}\omega_{agarose})$, with $C_{agarose}$ being the concentration of the polymer (w/v), $\rho_{agarose}$ being the density of dry agarose (1.64 g/mL), and $\omega_{agarose}$ being the mass fraction of agarose in a fiber, because of internally bound water (0.625, obtained from: Johnson, E. M.; Berk, D. A.; Jain, R. K.; Deen, W. M. *Biophys. J.* **1996**, *70*, 1017−1026.

(48) Mendes, E.; Lutz, P.; Bastide, J.; Boué, F. *Macromolecules* **1995**, *28*, 174−179.

(49) Griess, G. A.; Guiseley, K. B.; Serwer, P. *Biophys. J.* **1993**, *65*, 138−148.

(50) Martin, J. E.; Ackerson, B. J. *Phys. Rev. A* **1985**, *31*, 1180−1182.

(51) Bouchaud, E.; Delsanti, M.; Adam, M.; Daoud, M.; Durand, D. *J. Phys.* **1986**, *47*, 1273−1277.

(52) Martin, J. E. *J. Appl. Crystallogr.* **1986**, *19*, 25−27.

(53) The spherical cell model was tested, but it did not adequately fit $g^{SANS}(r)$.

(54) For eq 7, the assumption of negligible fiber thickness presents a problem because, in turn, it affects $\phi_{exc}(r_s=0)$, which should not be zero. $\phi_{exc}(r) = 1 - \int_r^\infty g(r)\, dr = 1 - \exp(-\alpha r^2)$ with $\alpha = (\pi/4\overline{r_p})$, and then a simple correction was made as follows and was applied in Figure 4a: $\phi_{exc}(r) = \phi + (1 - \phi)(1 - \exp(-\alpha r^2))$.

(55) Starchev, K.; Wilkinson, K.; Buffle, J. Applications of FCS of environmental systems. In *Topics in Fluorescence Spectroscopy, Techniques*; Lakowicz, J. R., Ed.; Plenum Press: New York, 1991; Vol. 1, pp 251−275.

(56) Starchev, K.; Buffle, J.; Perez, E. *J. Colloid Interface Sci.* **1999**, *213*, 479−487.

(57) Meseth, U.; Wohland, T.; Riegler, R.; Vogel, H. *Biophys. J.* **1999**, *76*, 1619−1631.

(58) Thompson, N.; Mitchell, J. L. High Order Autocorrelation in Fluorescence Correlation Spectroscopy. In *Fluorescence Sorrelation Spectroscopy*; Rigler, R., Elson, E. S., Eds.; Springer, Berlin, 2001; pp 439−458.